Stability of the current-carrying state in nonhomogeneous MgB_2 films

S. Treiber,* C. Stahl, and G. Schütz
Max-Planck-Institut für Intelligente Systeme, Heisenbergstr. 3, DE-70569 Stuttgart, Germany

J. Albrecht
Hochschule Aalen, Beethovenstr. 1, DE-73430 Aalen, Germany

(Received 3 August 2011; published 28 September 2011)

Superconducting thin films can get unstable against magnetic flux jumping. At low temperatures, the probability of an unstable critical state increases since a high critical current density leads to large gradients in the flux density distribution. This phenomenon is often referred to as magnetic flux avalanches. The formation and propagation of these avalanches can be extensively described using a thermomagnetic model. The description of the avalanche process gets more complex when the superconducting film is not homogeneous. Quantitative magneto-optical imaging at tailored MgB_2 films revealed that the stability of the current-carrying state is substantially reduced in inhomogeneous superconductors. This is closely related to flux focusing and increased electric fields.

DOI: 10.1103/PhysRevB.84.094533 PACS number(s): 74.25.Sv, 74.25.Wx, 74.70.Ad

I. INTRODUCTION

The current-carrying state in type II superconductors corresponds to an inhomogeneous vortex distribution in the material. At low temperatures where effective flux line pinning leads to large gradients in the vortex-density distribution, this state can get unstable. Kinematically driven vortex avalanches occur forming a different type of critical state.[1,2] This has in particular two consequences. Firstly, the integral critical current in the superconductor is drastically reduced because the pathways of the avalanches exhibit a vanishing critical current density and thus can not contribute to the current transport. Secondly, fast moving vortices during avalanche propagation[3,4] create an enormous amount of dissipated energy. At the same time, a huge amount of noise is created that, e.g., spoils the application as a magnetic sensor device. In case of MgB_2, this can affect the critical state below temperatures of about 10 K and brings out a disadvantage of the material.[5] On the other hand, MgB_2 exhibits several advantages compared to high-T_c materials such as the isotropic energy gap and the fact that grain boundaries are strong links.[6,7] Furthermore, MgB_2 is relatively easy to process and comparatively cheap.

The behavior of magnetic avalanches is described using a thermomagnetic model.[1,8] When heat conductivity falls below a critical value, thermal diffusion processes become too slow to remove the heat from the dissipative vortex motion.[9] Local heating then leads to an increased mobility of flux lines, the result is a positive feedback loop that forms dendrite-like flux patterns.[10]

Two mechanisms are known that intercept the loop. If the thermal conductivity of the system can be enhanced, the formation condition of avalanches is no longer given and an avalanche-free state develops. This can be achieved by covering the superconducting film with a metal layer such as Al or Au.[11] Also, during propagation of avalanches, eddy currents can be created in an adjacent layer of reasonable conductivity, which act as electromagnetic break.[12] As a consequence, it is necessary to distinguish between avalanche formation and propagation.[13]

Up to now, the description of magnetic avalanches only considers homogeneous superconductors. In this case, the process can be described by a single set of material parameters. We show that an extension to inhomogeneous superconductors such as granular or polycrystalline systems or even to patterned media requires an improved model. In particular, a nonlocal consideration of material constants is required to find a proper description.

II. EXPERIMENTAL DETAILS

MgB_2 films were prepared on r-cut Al_2O_3 substrates by sequential deposition of magnesium and boron layers using conventional electron beam evaporation and a subsequent annealing process.[14–16] These films have dimensions of 5×5 mm^2 and a thickness of 300 nm. Critical temperatures are typically 35 K and the current densities can exceed 1×10^{11}A/m^2 at 10 K. We achieved to prepare areas of different microstructures in one sample by an incomplete first evaporated Mg layer during deposition. As a consequence, some parts of the precursor exhibit a boron layer—instead of a magnesium layer—adjacent to the substrate after the complete sequential deposition. The areas where the precursor started with a layer of magnesium exhibit a smooth phase. The areas where the precursor has a bottom layer of boron develop during annealing into an inhomogeneous microstructure.[16]

Figure 1 shows a microscopy image of the sample and a magnification of the inhomogeneous area. It can be seen that there are regions of different optical contrast corresponding to areas of different precursor composition. The inner part (light gray) refers to a precursor composition having a substrate/magnesium interface. The outer area (dark gray) was generated from a precursor composition with a boron/substrate interface.

The two areas show different microstructures. The inner area is regular and smooth, while the surface of the outer area broke open during sample preparation. This led to the formation of cracks, which subdivide the sample into islands with diameters of about 30 μm. The typical structure is shown in the right panel of Fig. 1. It is important to note that the cracks visible at the surface do not reach the substrate. Since a transport supercurrent has to overcome these barriers, the

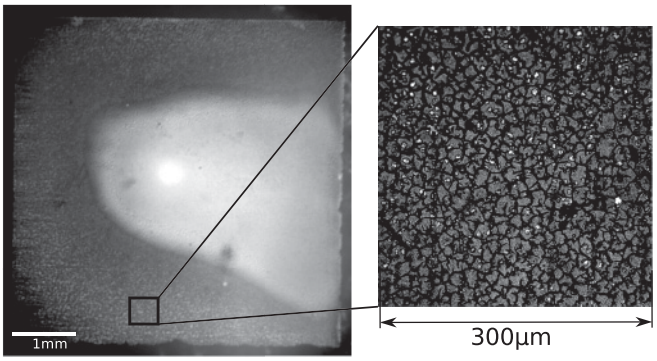

FIG. 1. Optical micrographs of the sample. The right image is a magnification of the inhomogeneous area of the sample that appears dark in the left image. The magnified image shows dark channels surrounding brighter "islands.' The critical current in the channels is about five times lower than in the islands.

overall measurable current on a length scale larger than the individual islands is determined by the limitation of the cracks. When an external field is applied to the sample, flux penetrates further inside these channels because the thickness of the superconductor is smaller. The islands, exhibiting a higher critical current I_c, remain flux free because larger screening currents shield the magnetic flux.

Owing to topological reasons, flux lines have to penetrate at the edge of the sample. This is important for the avalanche case as well.

The particular feature of our sample is that there are both inhomogeneous and regular regions at the edges of the sample. So it is possible to observe avalanche formation from the sample edge both in the inhomogeneous and in the regular areas. Additionally, avalanches, which are created in the inhomogeneous area, meet in the regular area while propagating. So, this kind of sample is suitable to gain a deeper understanding of both the avalanche propagation and formation processes in inhomogeneous MgB_2 thin films.

We used magneto-optical Faraday microscopy to map the flux-density distribution in the superconducting film. This is equivalent to the spatial density of vortices that have penetrated into the superconductor after having applied an external magnetic field. For this purpose, a magneto-optically active iron garnet film is placed on top of the sample. If an external field is applied, magnetic flux penetrates in the sample and consequently induces a magnetization in the garnet film. The garnet film is then illuminated with linear-polarized light, which leads to a rotation of the polarization axis depending on the local magnetization in the film. Images taken by a high sensitive CMOS camera show the distribution of magnetic flux in the superconducting structure. Additionally, a numerical inversion scheme of Biot-Savarts law provides a map of the current-density distribution in the sample.[17] This allows the determination of the density of supercurrents in the film with a spatial resolution of about 5 μm and high quantitative accuracy.

Figure 2 shows the magneto-optically obtained flux density distribution in the inhomogeneous film. The measurement was performed at $T = 12$ K. After zero-field cooling, an external field of $B_{\text{ext}} = 160$ mT has been applied and subsequently

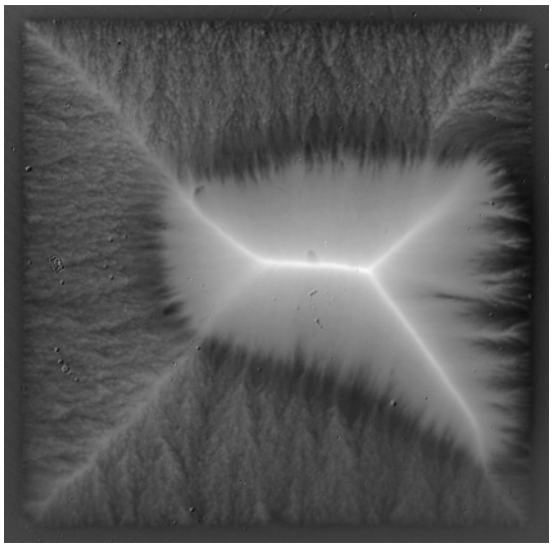

FIG. 2. Magneto-optical image showing the flux density distribution of the remanent state of the sample. This state was prepared by zero-field cooling the sample to $T = 12$ K. Then an external field of $B_{\text{ext}} = 160$ mT was applied and subsequently removed. Bright areas correspond to high flux density. It is clearly seen that the flux is smoothly distributed in the inner area, while the outer area exhibits a inhomogeneous flux density distribution.

removed. The so prepared remanent state exhibits the whole film being in the current-carrying critical state. The flux-density pattern is subdivided into two parts: a smooth region in the inner part and an inhomogeneous part around. The shape of both regions corresponds to the micrograph depicted in Fig. 1. The distortion of the white d lines directly indicates a nonhomogeneously distributed current density.[17,18]

III. FORMATION OF AVALANCHES

If the temperature is reduced to below $T = 10$ K, the critical state can get unstable and vortex movement can turn into a dynamically driven avalanche formation.[5] As a first step, we want to study the conditions for the formation of such avalanches in an inhomogeneous system. To describe the stability of a superconductor against macroscopic flux jumps, the dimensionless parameter $\tau = D_t/D_m = \mu_0\sigma\kappa/C$ is commonly used,[9] where σ is the electrical conductivity, κ is the thermal conductivity, and C is the specific heat. Flux jumps can take place when the thermal diffusivity D_t is much smaller than the magnetic diffusivity D_m, i.e., $\tau \ll 1$.[9] This means that the thermal transport is not fast enough to distribute the energy in the system. In general, all hard superconductors exhibit $\tau \ll 1$.[9] In superconducting thin films, the critical state is stable above an avalanche-formation temperature T_{af}. At $T < T_{\text{af}}$, large dendritic flux jumping, i.e., flux avalanches, can occur.

T_{af} strongly depends on the material. While T_{af} is clearly smaller than 1 K for YBCO single crystals,[19] in MgB_2 thin films, T_{af} is typically 10 K.[5,20,21] At this process, millions of vortices can penetrate the superconducting thin film in nanoseconds.[22] The conditions for avalanche formation in homogeneous superconducting thin films was described quantitatively by Denisov *et al.* in Ref. 1. Namely, there is

a threshold field $H_{\rm th}$ above which avalanches occur, which is given as

$$H_{\rm th} = \frac{I_c}{\pi}\operatorname{acosh}\left(\frac{w}{w-\ell^*}\right) \tag{1}$$

with

$$\ell^* = \frac{\pi}{2}\sqrt{\frac{\kappa T^* d}{I_c E}}\left(1-\sqrt{\frac{2h_0 T^*}{n I_c E}}\right)^{-1}. \tag{2}$$

Here, $I_c = j_c d$ is the sheet current, d is the thickness, w is the width of the sample, ℓ^* is the penetration depth above which the film becomes unstable, κ is the thermal conductivity, T^* is the characteristic of the temperature dependence of j_c obtained from $T^* = -(\partial \ln j_c/\partial T)^{-1}$, E is the electrical field, h_0 is the heat transfer coefficient to the substrate, and n is the exponent of the relation $E \propto j^n$. Note that Eq. (1) applies for an infinite slab, however, our qualitative discussion using the stability criterion of Eq. (2) also holds for thin squares.

Due to the the strong temperature dependence of κ and h_0,[23] $H_{\rm th}$ has a finite value only for $T < T_{\rm af}$. It also follows that a higher critical current density leads to a lower $H_{\rm th}$ and thus to a more unstable critical state. This behavior was found experimentally in Ref. 2 where the flux penetration behavior was observed in a MgB_2 sample with anisotropic current density. The investigated sample was square-shaped and exhibited a slightly higher j_c in one direction parallel to the rim. It was found, that at 10 K, avalanches only occur at the two rims parallel to the direction of higher j_c. This behavior can be explained by the large slope of the relation $H_{\rm th}(j_c)$ in the vicinity of $T_{\rm af}$.

Since the observed critical current is lower in the inhomogeneous area of our sample, one would expect, that avalanches prefer the high-current areas. However, this behavior is not seen, $H_{\rm th}$ is even much lower in the inhomogeneous areas. Figure 3(a) shows the critical current density distribution of the sample corresponding to the flux pattern in Fig. 2. This measurement illustrates the current-limiting properties of the microstructure of the inhomogeneous area. In the inner area, j_c values reach about $8 \times 10^{10}\mathrm{A/m^2}$ at $T = 12$ K. In the outer part, the observed currents are limited by the intersecting channels. The presented measurement shows the current density averaged over approximately 100 μm. Circulating currents in individual islands are not resolved. Figure 3(b) shows a magneto-optical measurement of the flux penetration into the inhomogeneous MgB_2 film at $B_{\rm ext} = 2.4$ mT and $T = 8$ K, which is below the avalanche formation temperature $T_{\rm af}$. Bright parts refer to a high local flux density. Magnetic flux penetrates into the film in form of dendrite-shaped flux avalanches. However, the avalanches only occur when formed at inhomogeneous parts at the edge of the sample. In Fig. 3(b), where the regular part (indicated by the dotted line) reaches the edge, no avalanches are formed.

This behavior can be explained when considering the microstructure-governed distribution of the critical current in the different regions of the film. In the inhomogeneous area, channels of low I_c surround islands exhibiting higher values of I_c. When an external magnetic field is applied, the penetration depth depends on the local critical current. Along the channels with reduced I_c, the vortices penetrate further into the film. At the same time, the penetrated flux creates eddy currents in the adjacent islands leading to an increase of the flux density inside the channels. This is called flux focusing effect.[17,24] This flux focusing can lead to local fields large enough to overcome the threshold field $H_{\rm th}$ for avalanche formation. Determining parameters are the local film characteristics inside the channel and the stray fields of adjacent islands. These depend on I_c in the islands and on the islands' size and shape. For a closed description of avalanche formation in an inhomogeneous superconducting film, the exact distribution of the superconducting properties has to be known and poses a huge nonlocal problem.

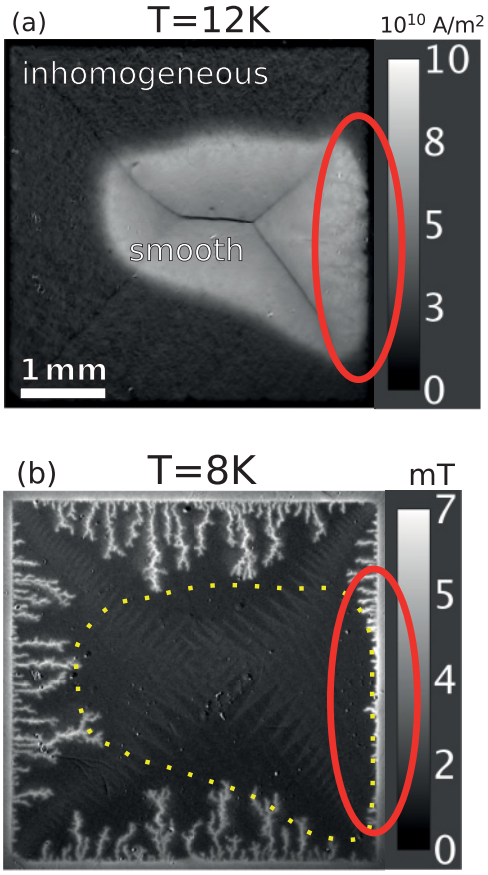

FIG. 3. (Color online) Current density distribution above $T_{\rm af}$ in the remanent state (a) and flux density distribution below $T_{\rm af}$ at $H_{\rm ext} = 2.4$ mT (b). The area where the rim of the sample is smooth is marked with a red oval. In (b), the dotted yellow line indicates the contour of the smooth area. It is clearly seen that avalanches form only in inhomogeneous areas.

A second effect has to be considered when describing flux penetration into inhomogeneous superconductors. When the flux penetration is inhomogeneous, local electrical fields appear that can be large.[8,18,25,26] In the avalanche-formation process, local heating plays an important role. One source of heat are normal-conducting currents, which depend on the electrical field following $j_{nc} = \sigma E$. Only a small amount of heat leads to a decrease of j_c (since $\frac{\partial j_c}{\partial T} < 0$). Consequently, the external field then penetrates further into the film and the moving flux creates even more heat and so on. The result can easily be an avalanche.

The combination of enhanced local flux density by flux focusing and the increased electrical field due to the irregular path of the current reduces the threshold field H_{th} and thus supports avalanche formation in the inhomogeneous area.

IV. PROPAGATION OF AVALANCHES

In this section, we investigate the influence of the inhomogeneous microstructure on the propagation of avalanches. The theory of avalanche propagation is so far the same as for formation. It is described in Ref. 1 by a thermomagnetic model that is based on the above mentioned stability criterion.[9] This model describes avalanche propagation as a consequence of local heating of the sample and the resulting mobility of flux lines. If the sample is not homogeneous, additional factors play a role. For example, arrays of antidots can influence the propagation direction.[27] Here, avalanches move from one antidot to another while short distances between two antidots are favored. This means that avalanches prefer an "easy" way using as much weak- or non-superconducting spots as possible. Another evidence for this behavior is found when an avalanche is created in the inhomogeneous area of our sample and then, while propagating, reaches a borderline to a smooth sample area. For not too large external fields, the result is that these avalanches stop immediately when the smooth area is reached.[13]

In this work, we compare the size and the shape of the avalanches and find a distinct difference for avalanches in inhomogeneous and smooth areas.

For this purpose, we applied an external field of $H_{\mathrm{ext}} = 3.2$ mT to the sample, which was initially zero-field cooled to $T_{\mathrm{af}} > T = 8$ K. Figure 4 shows two parts of one magneto-optical image of this state. Figure 4(a) shows a part of the inhomogeneous area while Fig. 4(b) shows a part of the smooth area. Both the size and the shape of the avalanches are completely different. While the avalanches in the inhomogeneous area are large with a lot of branching, avalanches in the smooth area are comparatively small and straight. Since these images represent the flux-density distribution, one can estimate the number of flux lines that form one avalanche. It

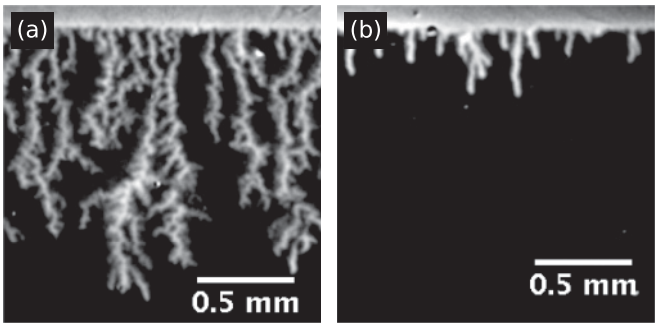

FIG. 4. Magneto-optical images of avalanches in two different areas. The figures are subimages of one magneto-optical image taken at $T = 8$ K and $H_{\mathrm{ext}} = 3.2$ mT. In the inhomogeneous area, one avalanche contains about ten times more flux lines than one avalanche in the smooth area. This finding supports the assumption that also the propagation of avalanches strongly depends on the microstructure.

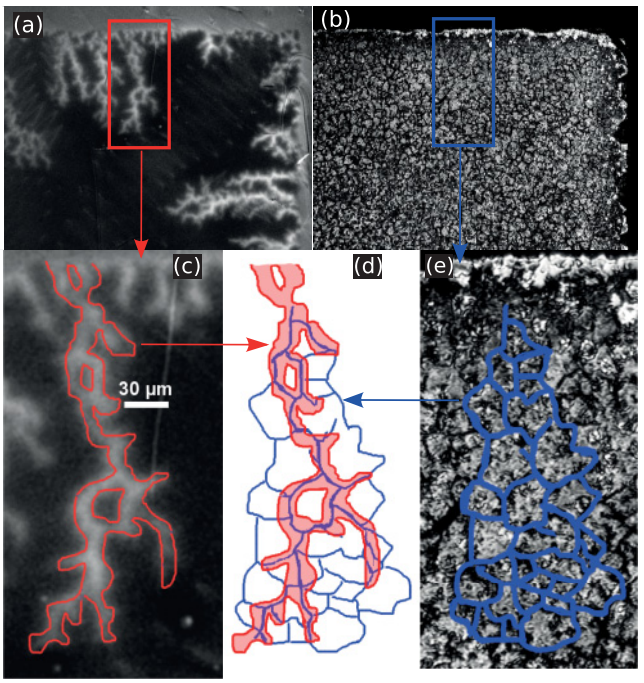

FIG. 5. (Color online) The images (c)–(e) show three different perspectives of a microscopy image (b) overlayed with a magneto-optical image (a) in order to illustrate propagation of avalanches in the inhomogeneous part of the sample. The red and blue rectangles in (a) and (b) correspond to the very same detail of the sample. (d) is an addition of the reference lines. It can be seen, that avalanches propagate in the channels of low j_c. The magneto-optical image is taken at $T = 8$ K and $B_{\mathrm{ext}} = 3.2$ mT.

was found that one avalanche under these conditions contains about $4 \times 10^4\ \Phi_0$ in the smooth area, while one avalanche in the inhomogeneous area contains about $4 \times 10^5\ \Phi_0$ with Φ_0 being the magnetic flux quantum. This large difference as well as the different shape can also be explained by the microstructure.

Microscopy images suggest that the low-I_c channels are thinner than the plates. This would mean the flux line energy is lower in the channels. This assumption is supported by our observations.

Figure 5 illustrates the propagation of magnetic flux avalanches in inhomogeneous structures showing three different perspectives [(c), (d), and (e)]. Figures 5(a) and 5(b) are a magneto-optical image and a micrograph of the very same detail of the sample. An area containing an avalanche was chosen from the magneto-optical image (c) and compared to the very same area of the micrograph (b). The colors (only seen online) were added to emphasize structures: red outlines the magnetic avalanche (c), and blue shows the platelike structure of the sample's surface (e). Figure 5(d) is a an overlay of the outlines. Due to the experimental setup with a magneto-optical layer on top of the sample, structures in magneto-optical images appear to be more blurred and broadened than they are in the sample underneath. Therefore the avalanche structure seems to be wider than the channel in the microscopy image, but this is not the case. The conclusion from these pictures is that the propagation of avalanches only takes place along channels of the sample surface structure. In these channels

of reduced thickness, the vortex self-energy has a minimum. Hence less energy is needed to drive forward the magnetic flux cores, and these structures are favored in the propagation of avalanches.

This leads to another general difference with avalanches in homogeneous media. In the case considered here, the pathway for the propagation of avalanches is not arbitrary like in homogeneous media.[28] Repeating a flux propagation experiment shows that avalanches choose not always the same way but they use low-I_c channels every time. A clear distinction, however, can be made when performing a magnetization measurement. Here, characteristic jumps in magnetization values occur when such avalanches are present. In particular, when concerning weak links and Josephson junctions where flux pinning is small and flux focusing large, the consideration of spatially confined avalanches might be important.

Since for many purposes, artificial structuring can turn plain superconducting films into structures of complex geometries, these findings may be important for the stability of the current-carrying state in some technical applications at very low temperatures.

V. CONCLUSION

We compared formation and propagation of magnetic flux avalanches in homogeneous and inhomogeneous MgB_2 thin films. For this purpose, we prepared samples containing smooth and granular areas at the same time. It was found that if the critical current I_c is distributed inhomogeneously, the critical state is much less stable. Spatially resolved magneto-optical measurements suggested three reasons. Firstly, areas of lower I_c can act as propagation channels for avalanches. Secondly, the areas of higher I_c provide large stray fields, which reduce the external threshold field H_{th}. Thirdly, an inhomogeneous current path leads to increased electrical fields, which support the dissipative avalanche process. The fact that inhomogeneities can lead to a collapse of the critical state might be an issue for artificially structured superconductors at very low temperatures.

*treiber@is.mpg.de

[1] D. V. Denisov, A. L. Rakhmanov, D. V. Shantsev, Y. M. Galperin, and T. H. Johansen, Phys. Rev. B **73**, 014512 (2006).

[2] J. Albrecht, A. T. Matveev, J. Strempfer, H.-U. Habermeier, D. V. Shantsev, Y. M. Galperin, and T. H. Johansen, Phys. Rev. Lett. **98**, 117001 (2007).

[3] M. R. Wertheimer and J. Gilchrist, J. Phys. Chem. Solids **28**, 2509 (1967).

[4] U. Bolz, B. Biehler, D. Schmidt, B.-U. Runge, and P. Leiderer, Europhys. Lett. **64**, 517 (2003).

[5] T. H. Johansen, M. Baziljevich, D. V. Shantsev, P. E. Goa, Y. M. Galperin, W. N. Kang, H. J. Kim, E. M. Choi, M.-S. Kim, and S. I. Lee, Supercond. Sci. Technol. **14**, 726 (2001).

[6] D. C. Larbalestier, L. D. Cooley, M. O. Rikel, A. A. Polyanskii, J. Jiang, S. Patnaik, X. Y. Cai, D. M. Feldmann, A. Gurevich, A. A. Squitieri, M. T. Naus, C. B. Eom, E. E. Hellstrom, R. J. Cava, K. A. Regan, N. Rogado, M. A. Hayward, T. He, J. S. Slusky, P. Khalifah, K. Inumaru, and M. Haas, Nature (London) **410**, 186 (2001).

[7] D. K. Finnemore, J. E. Ostenson, S. L. Bud'ko, G. Lapertot, and P. C. Canfield, Phys. Rev. Lett. **86**, 2420 (2001).

[8] R. G. Mints and E. H. Brandt, Phys. Rev. B **54**, 12421 (1996).

[9] R. G. Mints and A. L. Rakhmanov, Rev. Mod. Phys. **53**, 551 (1981).

[10] W. Desorbo and W. Healy, Cryogenics **4**, 257 (1964).

[11] M. Baziljevich, A. V. Bobyl, D. V. Shantsev, E. Altshuler, T. H. Johansen, and S. I. Lee, Physica C **369**, 93 (2002).

[12] F. Colauto, E. Choi, J. Y. Lee, S. I. Lee, E. J. Patino, M. G. Blamire, T. H. Johansen, and W. A. Ortiz, Appl. Phys. Lett. **96**, 092512 (2010).

[13] S. Treiber and J. Albrecht, New J. Phys. **12**, 093043 (2010).

[14] S. R. Shinde, S. B. Ogale, R. L. Greene, T. Venkatesan, P. C. Canfield, S. L. Bud'ko, G. Lapertot, and C. Petrovic, Appl. Phys. Lett. **79**, 227 (2001).

[15] A. T. Matveev, J. Albrecht, M. Konuma, B. Stuhlhofer, U. Starke, and H.-U. Habermeier, Supercond. Sci. Technol. **18**, 1313 (2005).

[16] A. T. Matveev, J. Albrecht, M. Konuma, G. Cristiani, Y. Krockenberger, U. Starke, G. Schütz, and H.-U. Habermeier, Supercond. Sci. Technol. **19**, 299 (2006).

[17] C. Jooss, J. Albrecht, H. Kuhn, S. Leonhardt, and H. Kronmüller, Rep. Prog. Phys. **65**, 651 (2002).

[18] T. Schuster, M. V. Indenbom, M. R. Koblischka, H. Kuhn, and H. Kronmüller, Phys. Rev. B **49**, 3443 (1994).

[19] R. J. Zieve, T. F. Rosenbaum, H. M. Jaeger, G. T. Seidler, G. W. Crabtree, and U. Welp, Phys. Rev. B **53**, 11849 (1996).

[20] Z. W. Zhao, S. L. Li, Y. M. Ni, H. P. Yang, Z. Y. Liu, H. H. Wen, W. N. Kang, H. J. Kim, E. M. Choi, and S. I. Lee, Phys. Rev. B **65**, 064512 (2002).

[21] T. H. Johansen, M. Baziljevich, D. V. Shantsev, P. E. Goa, Y. M. Galperin, W. N. Kang, H. J. Kim, E. M. Choi, M.-S. Kim, and S. I. Lee, Europhys. Lett. **59**, 599 (2002).

[22] D. V. Shantsev, A. V. Bobyl, Y. M. Galperin, T. H. Johansen, and S. I. Lee, Phys. Rev. B **72**, 024541 (2005).

[23] A. V. Sologubenko, J. Jun, S. M. Kazakov, J. Karpinski, and H. R. Ott, Phys. Rev. B **66**, 014504 (2002).

[24] P. A. Rosenthal, M. R. Beasley, K. Char, M. S. Colclough, and G. Zaharchuk, Appl. Phys. Lett. **59**, 3482 (1991).

[25] E. H. Brandt, Phys. Rev. B **52**, 15442 (1995).

[26] A. Gurevich and M. Friesen, Phys. Rev. B **62**, 4004 (2000).

[27] M. Kemmler, Ph.D. thesis, Universität Tübingen, 2008.

[28] J. Albrecht, P. Audehm, and M. Djupmyr, Supercond. Sci. Technol. **21**, 045016 (2008).